Eur. Phys. J. B **52**, 275–280 (2006)
DOI: 10.1140/epjb/e2006-00292-8

THE EUROPEAN PHYSICAL JOURNAL B

Applications of the expanded basis method to study the behavior of light in a two-dimensional photonic crystal slab

L.-M. Zhao and B.-Y. Gu[a]

Institute of Physics, Chinese Academy of Sciences, P.O. Box 603, Beijing 100080, P.R. China

Received 2 April 2006 / Received in final form 16 May 2006
Published online 31 July 2006 –

Abstract. We apply the expanded basis method (EBM) to investigate the behavior of light in a two-dimensional photonic crystal (PC) slab. This method is based on expanded completeness bases, including both the propagation and evanescence modes. We calculate the reflected and transmitted coefficients and the corresponding field distributions in the case of multiple mode transportation. We also show the related phases which exhibit oscillations with the frequency of the incident light.

PACS. 42.70.Qs Photonic bandgap materials – 42.25.Gy Edge and boundary effects; reflection and refraction – 42.68.Ay Propagation, transmission, attenuation, and radiative transfer – 42.25.Bs Wave propagation, transmission and absorption

1 Introduction

Photonic crystals (PCs), which possess spatially modulated dielectric structures, exhibit rich dispersion relations consisting of pass-bands and photonic band gaps (PBGs) [1,2]. Many novel phenomena induced by the PBGs have been revealed in perfect periodical structures [3–8]. However, a real sample always has a finite size and contains several interfaces, thus, the coupling between the incident light wave and the Bloch mode in PCs at interfaces should be considered.

A variety of theoretical or numerical methods have been proposed to study the behavior of light in finite-size PCs, for instance, the finite-difference time-domain (FDTD) technique, transfer matrix method (TMM), and multiple-scattering method (MSM), etc. Some methods based on a plane-wave expansion (PWE) of the electromagnetic (EM) field have been employed to calculate the reflection and transmission spectra of PC slabs [9–11]. Recently, Notomi [12] and Xu et al. [13] studied the behavior of the reflected light at a two-dimensional (2D) PC surface. Istrate et al. [14] discussed the reflection of light waves using the zeroth order Fourier component of the plane wave expansion at the interface of a finite size 2D PC based on the concept of effective refractive index (ERI) of a material. Yang et al. [15] studied the characteristics of the light propagation through a 2D PC slab with the use of the effective medium approximation based on equi-frequency surface calculations.

The expanded basis method (EBM) has been extensively adopted to study the transport properties of electrons in low-dimensional semiconductor quantum waveguides [16,17]. The calculation of the dispersion relation of electrons is usually attributed to solving the standard eigen equation, where only the propagating mode (with real wave number) is involved. By introducing auxiliary functions and rewriting in terms of an expanded basis set, the related problem can be recast into a framework of the generalized eigenvalue problem. The eigen wave number can then be real, imaginary, or complex. The EBM approach is a natural generalization of the original PWE method and it possesses several advantages: Firstly, it makes it easier to flexibly track and analyze the properties of various PCs including the loss materials; secondly, in the EBM the frequency is treated as a scanning variable, thus the value of frequency can always be set to be positive real even for complex systems with real (imaginary, or complex) frequency-dependent permittivity or permeability; thirdly, the resonant feature of transmittivity generated from the finite size of the PCs can be easily analyzed. Numerical simulations have demonstrated that the EBM is a more powerful and efficient method to track the above-addressed problems, compared to the conventional PWE method. This EBM has been proven to be appropriate for calculating the PBGs and reflectivity of semi-infinite 2D PCs [18–20].

In this work, we study the behavior of light in a two-dimensional (2D) PC slab with the use of the EBM, and strictly consider the interfacial matching conditions of electromagnetic (EM) fields. The specific expressions of the EM fields, including the reflected field, transmitted field, and internal field in the PC, can be acquired. Thus, the phases of the corresponding fields can be evaluated and they exhibit oscillations as a function of frequency.

[a] e-mail: guby@aphy.iphy.ac.cn

These phases dominate the interference patterns in the reflected and transmitted fields.

2 Expanded basis method for calculation of a photonic crystal slab

In an isotropic medium with spatially modulated permittivity $\epsilon(\mathbf{r})$ and permeability $\mu(\mathbf{r})$, according to the Maxwell equations, the magnetic field $\mathbf{H}(\mathbf{r})$ satisfies the following equation

$$\nabla \times \left[\frac{1}{\epsilon(\mathbf{r})}\nabla \times \mathbf{H}(\mathbf{r})\right] = \mu(\mathbf{r})\omega^2\mathbf{H}(\mathbf{r}). \quad (1)$$

As both $\epsilon(\mathbf{r})$ and $\mu(\mathbf{r})$ are periodic functions in the PCs, we can expand them and the magnetic (or electric) field in terms of a Fourier series as $\epsilon(\mathbf{r}) = \sum_{\mathbf{G}} \epsilon_{\mathbf{G}} e^{i\mathbf{G}\cdot\mathbf{r}}$, $\mu(\mathbf{r}) = \sum_{\mathbf{G}} \mu_{\mathbf{G}} e^{i\mathbf{G}\cdot\mathbf{r}}$, and $\mathbf{H}(\mathbf{r}) = \sum_{\mathbf{G}} \mathbf{H}_{\mathbf{G}} e^{i(\mathbf{k}+\mathbf{G})\cdot\mathbf{r}}$, where $\mathbf{G}$ denotes the reciprocal lattice vector; $\epsilon_{\mathbf{G}}$ and $\mu_{\mathbf{G}}$ are the Fourier expansion components of $\epsilon(\mathbf{r})$ and $\mu(\mathbf{r})$, respectively. ω and $\mathbf{k}$ are the frequency and wave vector, respectively.

In a 2D PC, the EM field equations can be decoupled from each other, therefore, two independent equations satisfied by the E-polarization (TM) (in-plane magnetic field) and H-polarization (TE) (in-plane electric field) modes read

$$\sum_{\mathbf{G}'} \mu^{-1}_{\mathbf{G}-\mathbf{G}'}(\mathbf{k}+\mathbf{G})\cdot(\mathbf{k}+\mathbf{G}')\mathbf{E}_{\mathbf{k},\mathbf{G}'} = \omega^2 \sum_{\mathbf{G}'} \epsilon_{\mathbf{G}-\mathbf{G}'}\mathbf{E}_{\mathbf{k},\mathbf{G}'} \quad (2)$$

for the TM mode and

$$\sum_{\mathbf{G}'} \epsilon^{-1}_{\mathbf{G}-\mathbf{G}'}(\mathbf{k}+\mathbf{G})\cdot(\mathbf{k}+\mathbf{G}')\mathbf{H}_{\mathbf{k},\mathbf{G}'} = \omega^2 \sum_{\mathbf{G}'} \mu_{\mathbf{G}-\mathbf{G}'}\mathbf{H}_{\mathbf{k},\mathbf{G}'}, \quad (3)$$

for the TE mode.

We can rewrite equation (2) as

$$\sum_{\mathbf{G}'\mathbf{G}''} \epsilon^{-1}_{\mathbf{G}-\mathbf{G}''}\mu^{-1}_{\mathbf{G}-\mathbf{G}''}(\mathbf{k}+\mathbf{G}')\cdot(\mathbf{k}+\mathbf{G}'')\mathbf{E}_{\mathbf{k},\mathbf{G}''} = \omega^2\mathbf{E}_{\mathbf{k},\mathbf{G}}, \quad (4)$$

where we have used $\sum_{\mathbf{G}} \epsilon_{\mathbf{G}''-\mathbf{G}}\epsilon^{-1}_{\mathbf{G}-\mathbf{G}'} = \delta(\mathbf{G}''-\mathbf{G}')$.

Equation (4) belongs to a standard eigen equation when both permittivity and permeability are real and frequency-independence. In this case, to obtain the dispersion spectrum of an infinitely extended periodic system, we usually scan the wave vector along the boundaries of the first Brillouin zone (FBZ) to calculate the corresponding eigen frequency through equation (4). However, when the permittivity and permeability of materials in PCs are complex or frequency-dependent, equation (4) no longer corresponds to an eigen value problem. Consequently, it is impossible to utilize the well-developed programming packages for solving standard eigen equations to obtain the dispersions of the PCs. However, by introducing auxiliary functions and using expanded bases, the problem can be rewritten as an eigenvalue problem formally. For different cases, there are two techniques: One technique is that we initially fix the direction of the wave vector along the boundaries of the FBZ and scan the frequency to find the magnitude of the wave number by solving equation (2); the second method is that we initially fix one of the components of the wave vector, for instance, $k_x = 0.5(2\pi/a)$ when calculating the dispersion spectrum in a 2D square lattice PC (with lattice a) along the X to M wave vector direction in the FBZ (or $k_y = 0$ when calculating the dispersion spectrum along the Γ to X direction). We then scan the frequency to find another unknown component of the wave vector, k_y (or k_x). The band structures can ultimately be obtained in this way.

For the first technique, we reformulate equation (2) as

$$\sum_{\mathbf{G}'} \mu^{-1}_{\mathbf{G}-\mathbf{G}'}[k^2 + k\hat{\mathbf{k}}\cdot(\mathbf{G}+\mathbf{G}') + \mathbf{G}\cdot\mathbf{G}']\mathbf{E}_{\mathbf{G}'} = \omega^2 \sum_{\mathbf{G}'} \varepsilon_{\mathbf{G}-\mathbf{G}'}\mathbf{E}_{\mathbf{G}'}$$

for the TM modes. Applying the formulas of

$$\sum_{\mathbf{G}} \mu_{\mathbf{G}''-\mathbf{G}}\mu^{-1}_{\mathbf{G}-\mathbf{G}'} = \delta\left(\mathbf{G}''-\mathbf{G}'\right)$$

and

$$\sum_{\mathbf{G}} \epsilon_{\mathbf{G}''-\mathbf{G}}\epsilon^{-1}_{\mathbf{G}-\mathbf{G}'} = \delta\left(\mathbf{G}''-\mathbf{G}'\right)$$

to both sides, we then obtain

$$\begin{pmatrix} 0 & \hat{\mathbf{I}} \\ \hat{\mathbf{R}} & \hat{\mathbf{S}} \end{pmatrix}\begin{pmatrix} \mathbf{E}_{\mathbf{G}'} \\ k\mathbf{E}_{\mathbf{G}'} \end{pmatrix} = k\begin{pmatrix} \mathbf{E}_{\mathbf{G}} \\ k\mathbf{E}_{\mathbf{G}} \end{pmatrix}, \quad (5)$$

where

$$\hat{\mathbf{R}} = \sum_{\mathbf{G}''} \mu_{\mathbf{G}-\mathbf{G}''}\left[\omega^2\epsilon_{\mathbf{G}''-\mathbf{G}'} - \mu^{-1}_{\mathbf{G}''-\mathbf{G}'}\mathbf{G}''\cdot\mathbf{G}'\right],$$
$$\hat{\mathbf{S}} = -\sum_{\mathbf{G}''} \mu_{\mathbf{G}-\mathbf{G}''}\left[\mu^{-1}_{\mathbf{G}''-\mathbf{G}'}\hat{\mathbf{k}}\cdot\left(\mathbf{G}''+\mathbf{G}'\right)\right].$$

Here $\hat{\mathbf{I}}$ represents a unit matrix $\{\delta_{\mathbf{G},\mathbf{G}'}\}$ and $\hat{\mathbf{k}}$ denotes the unit directional vector of $\mathbf{k}$. Similarly, we can derive the corresponding equation for the TE modes, just by performing simple exchange of the permittivity and permeability as well as the replacement of electric field by magnetic field in equation (5).

Regarding to the second method, we initially fix one of the components of the wave vector, k_x (or k_y), and then scan the frequency to find another unknown component of wave vector, k_y (or k_x). For instance, when k_y is initially fixed, and scanning ω to find k_x, equation (2) can then be rewritten as

$$\begin{pmatrix} 0 & \widehat{\mathbf{I}} \\ \widehat{\mathbf{P}} & \widehat{\mathbf{Q}} \end{pmatrix}\begin{pmatrix} \mathbf{E}_{\mathbf{G}'} \\ k_x\mathbf{E}_{\mathbf{G}'} \end{pmatrix} = k_x\begin{pmatrix} \mathbf{E}_{\mathbf{G}} \\ k_x\mathbf{E}_{\mathbf{G}} \end{pmatrix}, \quad (6)$$

where

$$\widehat{\mathbf{P}} = \sum_{\mathbf{G}''} \mu_{\mathbf{G}-\mathbf{G}''} \Big[\omega^2 \epsilon_{\mathbf{G}''-\mathbf{G}'} - \mu^{-1}_{\mathbf{G}''-\mathbf{G}'} . (\mathbf{G}^{''} + k_y \widehat{y}) \cdot (\mathbf{G}^{'} + k_y \widehat{y}) \Big],$$

$$\widehat{\mathbf{Q}} = -\sum_{\mathbf{G}''} \mu_{\mathbf{G}-\mathbf{G}''} \left[\mu^{-1}_{\mathbf{G}''-\mathbf{G}'} (\mathbf{G}^{''}_x + \mathbf{G}^{'}_x) \right].$$

Here $\widehat{y}$ denotes the unit vector in the y-direction.

In analogy to the above procedure, in the case of initially fixed k_x and scanning ω, the corresponding equation to determine k_y can also be obtained. The corresponding eigen equation has a similar form with the above equation except for exchanging k_y and k_x with each other. It is worth pointing out that in equation (5) (or Eq. (6)) we have extended the original basis of $\{\mathbf{E}_{\mathbf{G}'}\}$ to a set of expanded bases of $\{\mathbf{E}_{\mathbf{G}'}, k\mathbf{E}_{\mathbf{G}'}\}$ (or $\{\mathbf{E}_{\mathbf{G}'}, k_x\mathbf{E}_{\mathbf{G}'}\}$). The matrix on the left-hand side of equation (5) (or Eq. (6)) now no longer persists Hermiticity. Therefore, equation (5) (or Eq. (6)) corresponds to a pseudo-eigenvalue problem with complex eigenvalues of k (or k_x). The wave functions in the expanded bases correspond to the propagation (with real k) or evanescence modes (with complex k). By simply exchanging the permittivity and permeability tensors, as well as replacing the electric field by the magnetic field, the analogue equation to equation (6) for the TE modes can easily be derived.

Now, we investigate the transmissivity and reflectivity of light in a 2D PC slab which is located at region II and surrounded by dielectric medium on either side (referred to as regions I and III), as shown in Figure 1. The PC consists of a square lattice (with lattice constant a) of holes (with radius s). The slab thickness direction denotes the x-axis; the periodic plane layers are laid on the yz plane and holes are etched in the medium along the z-direction. We assume that a plane light wave is launched upon the surface of the PC slab from its left-side. The gray, dotted, and black arrows indicate the directions of the wave vectors of the incident, reflected, and transmitted waves, respectively. The coordination of the center of the holes in the first layer of the 2D PC slab is chosen to be $x = 0$; therefore, the interface between regions I and II (or regions II and III) is positioned at $x_1 = -s$ (or $x_3 = (N-1)a+s$). Here N represents the number of periodic plane layers in the PC slab. When using the incident plane wave with $E_{in} = E_0 e^{i[k_{(in),x}(x-x_1)+k_{(in),y}y]}$ to illuminate the 2D PC, a set of real or complex Bloch modes may be excited. The EM field in region I is a superposition of the incident plane wave and the reflected Bragg waves, whereas in region III, the EM field only contains the transmitted Bragg waves by considering the scattering condition. For instance, the electric fields of the TM mode

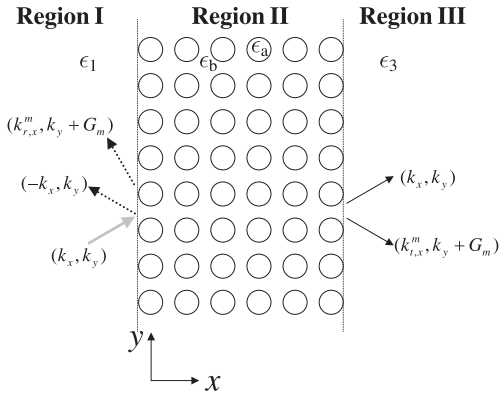

Fig. 1. Schematic view of the system considered in this paper. A 2D PC slab with a finite thickness is located at region II and surrounded by dielectric medium on both sides (denoted as regions I and III). The PC consists of a square lattice (with a lattice constant a) of air holes (with radius s). The periodic plane layers are laid on the yz plane and holes are etched along the z-direction; the thickness of the PC slab is along the x-direction. A plane light wave is launched upon the surface of the PC slab from its left-hand side. The gray, dotted, and black arrows indicate the directions of the wave vectors for the incident, reflected, and transmitted waves, respectively. The coordination of the center of the air holes in the first periodic plane layer of the 2D PC slab sets $x = 0$. The dielectric constants of holes and background medium are denoted by ϵ_a and ϵ_b, and the dielectric constants of medium in region I and III are denoted as ϵ_1 and ϵ_3, respectively.

in regions I and III read as

$$E_1(x,y) = E_0 e^{i[k_{(in),x}(x-x_1)+k_{(in),y}y]} + \sum_n r_n e^{i[k^{(n)}_{r,x}(x-x_1)+k^{(n)}_{r,y}y]}, \quad (7)$$

$$E_3(x,y) = \sum_n t_n e^{i[k^{(n)}_{t,x}(x-x_3)+k^{(n)}_{t,y}y]}. \quad (8)$$

We have $k_{(in),y} = k_y + m(\frac{2\pi}{a})$ and k_y is limited in the FBZ. The wave vectors of the nth order reflected and transmitted Bragg modes are given by $k^{(n)}_{r,y} = k^{(n)}_{t,y} = k_y + G_n$ with $G_n = 2\pi n/a$ $(n = 0, \pm1, \pm2, ...)$; $k^{(n)}_{r,x} = \sqrt{\epsilon_1(\omega/c)^2 - (k^{(n)}_{r,y})^2}$ and $k^{(n)}_{t,x} = \sqrt{\epsilon_3(\omega/c)^2 - (k^{(n)}_{t,y})^2}$; ϵ_1 (ϵ_3) is the dielectric constant of medium in region I (III). Note that $k^{(n)}_{r,x}$ or $k^{(n)}_{t,x}$ may be imaginary, corresponding to the decay reflected or transmitted Bragg modes, which have no contribution to reflectivity or transmissivity. The electric field in region II can be written as a superposition of the Bloch modes

$$E_2(x,y) = \sum_{\alpha=b,f} \sum_j C^{(\alpha)}_j \sum_{\mathbf{G}} \mathbf{E}^{(\alpha),j}_{\mathbf{G}} e^{i[(k^{(\alpha)}_{j,x}+G_x)x+(k_y+G_y)y]}, \quad (9)$$

where $\mathbf{G} = G_x\widehat{x} + G_y\widehat{y}$; $k^{(b)}_{j,x}$ ($k^{(f)}_{j,x}$) represents the wave vector of the jth backward (forward) propagating Bloch wave. Employing the matching technique, the electric fields at the interface between region I and II, or at the interface

between region II and III, should satisfy the following equations:

$$\begin{aligned} E_1(x_1,y) &= E_2(x_1,y), \\ E_2(x_3,y) &= E_3(x_3,y), \\ \frac{\partial}{\partial x}E_1(x,y)|_{x_1} &= \frac{\partial}{\partial x}E_2(x,y)|_{x_1}, \\ \frac{\partial}{\partial x}E_2(x,y)|_{x_3} &= \frac{\partial}{\partial x}E_3(x,y)|_{x_3}. \end{aligned} \tag{10}$$

Substituting equations (7–9) into equation (10), we obtain

$$\widehat{\mathbf{A}}\begin{pmatrix} \widehat{r} \\ \widehat{C}^{(b)} \\ \widehat{C}^{(f)} \\ \widehat{t} \end{pmatrix} = \begin{pmatrix} \widehat{E}_{in} \\ \widehat{0} \\ k_x\widehat{E}_{in} \\ \widehat{0} \end{pmatrix}. \tag{11}$$

Here, we denote $\widehat{r} = (r_1, r_2, ...r_{N_y})^T$, $\widehat{t} = (t_1, t_2, ...t_{N_y})^T$, $\widehat{E}_{in} = (0, ..., E_0, 0, ...)^T$, and $\widehat{E}_{in}$ only has one nonzero element E_0 when $G_y = m(\frac{2\pi}{a})$. $\widehat{C}^{(b)} = (C_1^{(b)}, C_2^{(b)}, ..., C_{N_y}^{(b)})^T$, $\widehat{C}^{(f)} = (C_1^{(f)}, C_2^{(f)}, ..., C_{N_y}^{(f)})^T$, N_y denotes the number of y-components of plane waves in the expansions. The symbol 'T' in the superscript represents the transposition of a row vector to a column vector. The matrix $\widehat{A}$ can then be written as

$$\widehat{\mathbf{A}} = \begin{pmatrix} -\widehat{I} & \widehat{S}_1^{(I)} & \widehat{S}_2^{(I)} & \widehat{0} \\ 0 & \widehat{S}_1^{(III)} & \widehat{S}_2^{(III)} & \widehat{I} \\ \widehat{K}^{(r)} & \widehat{S}_3^{(I)} & \widehat{S}_4^{(I)} & \widehat{0} \\ \widehat{0} & \widehat{S}_3^{(III)} & \widehat{S}_4^{(III)} & \widehat{K}^{(t)} \end{pmatrix}. \tag{12}$$

The elements of $\widehat{S}_{1(2,3,4)}^{(l)}$ are

$$S_1^{(l)}(m,j) = \sum_{G_x} \mathbf{E}_{G_x,G_m}^{(b),j} e^{i(k_{j,x}^{(b)}+G_x)x_l}, \tag{13a}$$

$$S_2^{(l)}(m,j) = \sum_{G_x} \mathbf{E}_{G_x,G_m}^{(f),j} e^{i(k_{j,x}^{(f)}+G_x)x_l}, \tag{13b}$$

$$S_3^{(l)}(m,j) = \sum_{G_x} \left(k_{j,x}^{(b)} + G_x\right) \mathbf{E}_{G_x,G_m}^{(b),j} e^{i(k_{j,x}^{(b)}+G_x)x_l}, \tag{13c}$$

$$S_4^{(l)}(m,j) = \sum_{G_x} \left(k_{j,x}^{(f)} + G_x\right) \mathbf{E}_{G_x,G_m}^{(f),j} e^{i(k_{j,x}^{(f)}+G_x)x_l}, \tag{13d}$$

where (l = I, III), $x_I = x_1$ and $x_{\mathrm{III}} = x_3$. $\widehat{K}^{(r)}$ (or $\widehat{K}^{(t)}$) represents a diagonal matrix consisting of the matrix elements of $k_{r,x}^{(n)}$ (or $k_{t,x}^{(n)}$). There are several consequences of this method that are important to note. (i) The perfect periodicity is broken and the evanescent modes can be generated for a finite PC. Using the conversional eigen equation shown in equation (4), it is difficult to find the evanescent modes as it belongs to a problem for seeking real eigen frequency solutions with an imaginary Bloch wave number. However, by expanding the original basis $\{\mathbf{E_G}\}$ to the expanded bases of $\{\mathbf{E_G}, k_x\mathbf{E_G}\}$ in equation (6), the eigen functions in the expanded bases contain both the propagating and evanescence modes. (ii) In the EBM, the frequency is treated as the scanning variable, therefore, making it easy to tackle the complex system with real (imaginary, or complex) frequency-dependent permittivity or permeability. (iii) The EBM can be applied to treat various PC structures with arbitrary shaped scatterers and any kind of lattices of 2D PCs.

3 Results and analysis

To compute the transmission and reflection coefficients, we have to first decide the direction of the Poynting vector of every mode. When the Bloch wave vector is real, the direction of the Poynting vector should be along the $\pm x$ direction for the forward/backward Bragg waves. However, when the Bloch wave vector is complex, from the physical consideration, the forward (or backward) Bragg waves should correspond to $\mathrm{Im}(k_x) > 0$ (or $\mathrm{Im}(k_x) < 0$). The transmittance T and reflectance R can be calculated from $\{r_n\}$ and $\{t_n\}$; the accuracy is estimated by the derivation value of $R + T$ from unity.

We next determine the behavior of light propagation in a 2D PC slab. The PC slab is composed of a square lattice of air holes with radius $r = 0.35a$. The dielectric of the background is $\epsilon_b = 12.0$ and the dielectric constant of the medium in regions I and III is the same as $\epsilon_1 = \epsilon_3 = 12.0$. The PC slab contains six periodic plane layers. We calculate the reflection and transmission coefficients through strictly solving the field equations including the high order Bragg modes. We reexpress the reflection (transmission) coefficient as: $r_n = |r_n|\exp(i\phi_n^{(r)})$ ($t_n = |t_n|\exp(i\phi_n^{(t)})$) where $|r_n|$ ($|t_n|$) denotes the amplitude and $\phi_n^{(r)}$ ($\phi_n^{(t)}$) is the phase of the reflection (transmission) coefficient of the jth order Bragg mode.

The variations of the amplitude and phase of the reflection (transmission) coefficient as a function of frequency are depicted in Figure 2: (a) $\phi_{0,\pm1}^{(r)}$, (b) $|r_{0,\pm1}|$, (c) $\phi_{0,\pm1}^{(t)}$, and (d) $|t_{0,\pm1}|$, corresponding to the zeroth order Bragg mode (solid curves) and the ±1-order Bragg modes (dotted curves). Two contiguous curves have been shifted vertically by -0.2 for the amplitude plot (or -0.25π for the phase plot) for clarity. It is clearly seen that when $\omega < 0.2887(2\pi c/a)$, only the zero-order Bragg reflected (transmitted) wave is excited, i.e., a propagating mode; it contributes to reflectivity (transmissivity). However, the first order Bragg reflected (transmitted) wave becomes a propagating mode when $\omega > 0.2887(2\pi c/a)$ and their amplitude is now comparable with that of the zero-order Bragg mode. This shows that the higher order Bragg reflected (transmitted) waves become important components and they cannot be neglected. Owing to the conservation of wave vectors of fields in the structure, the Bragg reflected (transmitted) wave vector should satisfy the following condition: $k_{r,y}^{(n)} = k_y + G_n$ ($k_{t,y}^{(n)} = k_y + G_n$). When $k_{r,y}^{(n)} \le \sqrt{\epsilon_1}\omega/c$ ($k_{t,y}^{(n)} \le \sqrt{\epsilon_3}\omega/c$), the Bragg reflected (transmitted) waves correspond to the propagating

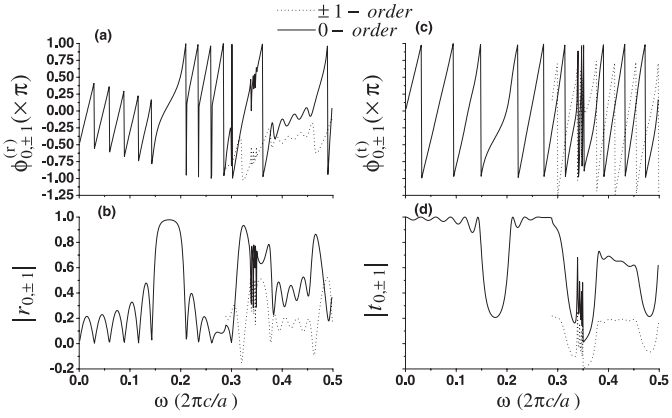

Fig. 2. Variations of phase and amplitude of the reflection (transmission) coefficient as a function of the frequency for the zero-order (solid curves) and the ±1-order (dotted curves) Bragg modes in the normal incidence of light: (a) $\phi^{(r)}_{0,\pm1}$, (b) $|r_{0,\pm1}|$, (c) $\phi^{(t)}_{0,\pm1}$, and (d) $|t_{0,\pm1}|$. Two consecutive curves in the phase- (or amplitude-) plot have been vertically shifted by an amount of -0.25π (or -0.2) for clarity.

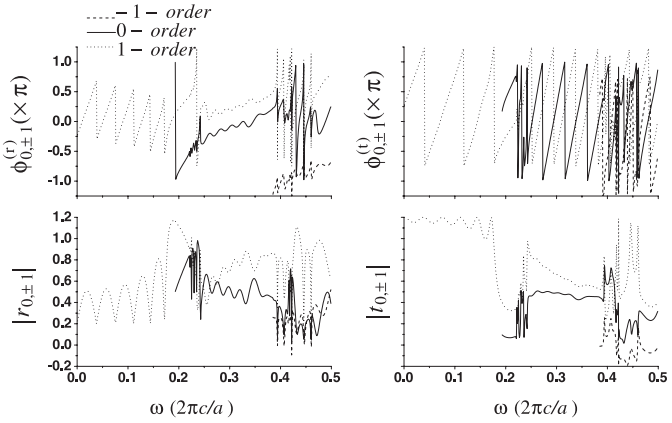

Fig. 3. Variations of phase and amplitude of the reflection (transmission) coefficient as a function of the frequency for the zero-order (solid curves), the ±1-order (dotted/dashed curves) Bragg modes in the oblique incidence of light at an angle of 30°: (a) $\phi^{(r)}_{0,\pm1}$, (b) $|r_{0,\pm1}|$, (c) $\phi^{(t)}_{0,\pm1}$, and (d) $|t_{0,\pm1}|$. Two consecutive curves in the phase- (or amplitude-) plot have been vertically shifted by an amount of $\pm0.25\pi$ (or ±0.2) for clarity.

modes and contribute to transmissivity (reflectivity). However, if $k^{(n)}_{r,y} > \sqrt{\epsilon_1}\omega/c$ ($k^{(n)}_{t,y} > \sqrt{\epsilon_3}\omega/c$), the Bragg reflected (transmitted) waves become the decay modes, consequently, they do not contribute to transmissivity (reflectivity). It is apparent from Figure 2 that the reflection coefficient exhibits oscillations in the extended band. In the frequency range of $\omega < 0.2887(2\pi c/a)$, only the zero-order Bragg mode is the propagating mode and the smallest reflected amplitude approaches zero at some frequencies where the corresponding phase produces a π-jump. These oscillation structures originate from the finite number of periodic plane layers in the PC slab, which can be regarded as an effective medium. For some frequencies, the phases of transmitted waves become the same after the transmitted waves experience the repeated reflection at the boundaries, therefore, the amplitude of the transmitted light will be increased rapidly. This is the so-called resonant transmission. In this case, the amplitude of the reflected light reaches zero and its real part and imaginary part change their signs correspondingly. Thus, the phase undergoes a π-jump at resonant frequency. When ±1-order Bragg modes participate in the transport process, the variation of phase in the reflection (transmission) coefficient with frequency exhibits continuous change for both the zero order and ±1-order Bragg modes, the effect of resonant transmission becomes non-obvious in this case.

Figure 3 shows the variations of the phases and the magnitudes of the reflection and transmission coefficients with frequency when the light lands obliquely on the PC slab at an angle of 30°: (a) $\phi^{(r)}_{0,\pm1}$, (b) $|r_{0,\pm1}|$, (c) $\phi^{(t)}_{0,\pm1}$, and (d) $|t_{0,\pm1}|$, corresponding to the zeroth order Bragg mode (solid curves), the ±1-order Bragg modes (dotted/dashed curves). The other parameters remain the same as those in Figure 2. Two consecutive curves have been vertically displaced by ±0.2 in the amplitude plot (or $\pm0.25\pi$ in the phase plot) for clarity. The reflection (transmission) coefficients are not equal for the ±1-order Bragg modes, unlike the case of normal incident of the light. It is clearly seen that when $\omega < 0.1925(2\pi c/a)$, only the +1-order Bragg reflected (transmitted) wave is excited, contributing to reflectivity (transmissivity). However, the zero order Bragg reflected (transmitted) wave is excited when $\omega > 0.1925(2\pi c/a)$, and the −1-order Bragg reflected (transmitted) wave becomes a propagating mode when $\omega > 0.3850(2\pi c/a)$. When $\omega < 0.1925(2\pi c/a)$, the smallest reflected amplitude approaches zero at some frequencies where the corresponding phase exhibits a π-jump. For $\omega > 0.1925(2\pi c/a)$, the phase of the reflection (transmission) coefficient exhibits a continuous change.

The distributions of the reflected or transmitted fields at $\omega = 0.4(2\pi c/a)$ in a specified space are displayed in Figure 4: (a) for the reflected field in region I and (b) for the transmitted field in region III. The parameters are chosen to be the same as those in Figure 2. If only the zero-order Bragg wave is excited, for example, when $\omega < 0.2887(2\pi c/a)$, the reflected (transmitted) wave takes a form of the plane wave. In contrast, when $\omega > 0.2887(2\pi c/a)$, besides the zero-order Bragg mode, the higher order Bragg modes also participate in the transport process in region I or III. They interfere with each other and generate an interference pattern, as shown in Figure 4.

4 Summary

In summary, we calculate the reflection and transmission coefficients of light in a 2D PC slab, composed of a square lattice of air holes, with the use of the expanded basis method (EBM) and the matching technique. We examine the variations of the amplitude and phase of the reflection (transmission) coefficient as a function of frequency. It is

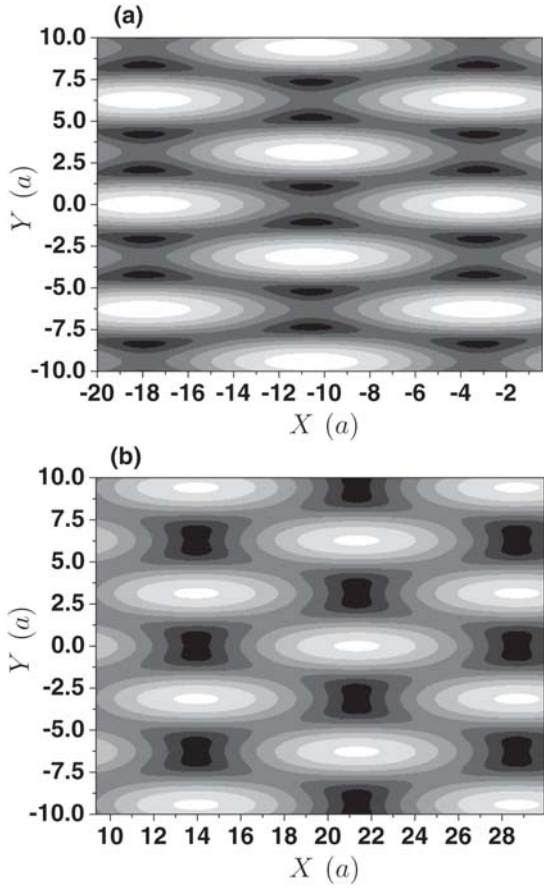

Fig. 4. Field distributions in a specified space when $\omega = 0.4(2\pi c/a)$, (a) for the reflected field in region I and (b) for the transmitted field in region III.

found that the excitation of the Bragg modes in the PC slab crucially depends on the frequency of the incident light wave and the incident angle. In some frequency regions, the higher order Bragg reflected (transmitted) modes become important components and have significant contribution to the transmissivity (reflectivity). The reflection coefficient exhibits oscillations in the extended band. We also show the distributions of the reflected or transmitted fields in the case of multiple mode transportation. When multiple Bragg modes participate in the transport process, they interfere with each other and generate an interference pattern.

This work was supported by the Chinese National Key Basic Research Special Fund under Grant No. 2001CB610402.

References

1. E. Yablonovitch, Phys. Rev. Lett. **58**, 2059 (1987)
2. S. John, Phys. Rev. Lett. **58**, 2486 (1987)
3. Xue-Hua Wang, Rongzhou Wang, Ben-Yuan Gu, Guo-Zhen Yang, Phys. Rev. Lett. **88**, 093902 (2002)
4. Rongzhou Wang, Xue-Hua Wang, Ben-Yuan Gu, Guo-Zhen Yang, Phys. Rev. B **67**, 155114 (2003)
5. E. Chow, S.Y. Lin, S.G. Johnson, P.R. Villeneuve, J.D. Joannopoulos, J.R. Wendt, G.A. Vawter, W. Zubrzycki, H. Hou, A. Alleman, Nature **407**, 983 (2000)
6. D.R. Smith, S. Shultz, N. Kroll, M. Sigalas, K.M. Ho, C.M. Soukoulis, Appl. Phys. Lett. **65**, 645 (1994)
7. Yun-Song Zhou, Ben-Yuan Gu, Fu-He Wang, J. Phys.: Condens. Matter **15**, 4109 (2003)
8. R.Z. Wang, X.H. Wang, B.Y. Gu, G.Z. Yang, J. Appl. Phys. **90**, 4307 (2001)
9. K. Sakoda, Phys. Rev. B **51**, 4672 (1995)
10. K. Sakoda, Phys. Rev. B **52**, 8992 (1995)
11. Zhi-Yuan Li, Kai-Ming Ho, Phys. Rev. B **68**, 155101 (2005)
12. M. Notomi, Phys. Rev. B **62**, 10696 (2000)
13. Xiao-Fang Xu, Shang-Hui Fan, Phys. Rev. E **70**, 055601 (2004)
14. E. Istrate, A.A. Green, E.H. Sargent, Phys. Rev. B **71**, 195122 (2005)
15. Suxia Yang, Tao Xu, H. Ruda, Phys. Rev. B **72**, 075128 (2005)
16. S. Chaudhuri, S. Bandyopadhyay, J. Appl. Phys. **71**, 3027 (1992)
17. Ben-Yuan Gu, Yuh-Kae Lin, Der-San Chuu, J. Appl. Phys. **86**, 1013 (1999)
18. Young-Chung Hsue, Tzong-Jer Yang, Sol. Stat. Comm. **129**, 475 (2004)
19. Young-Chung Hsue, Tzong-Jer Yang, Phys. Rev. E **70**, 016706 (2004)
20. Young-Chung Hsue, A.J. Freeman, Ben-Yuan Gu, Phys. Rev. B **72**, 195118 (2005)